Digest Journal of Nanomaterials and Biostructures Vol. 8, No. 1, January – March 2013, p. 167 - 176

THE EFFECT OF HEAT TREATMENT ON PHASE TRANSFORMATION, MORPHOLOGY AND PHOTOELECTROCHEMICAL RESPONSE OF SHORT TiO_2 NANOTUBES

YING-CHIN LIM[a,d], ZULKARNAIN ZAINAL[a, b*], MOHD ZOBIR HUSSEIN[a, b],
WEE-TEE TAN[c]
[a]*Centre of Excellence for Catalysis Science and Technology, Department of Chemistry, Faculty of Science, Universiti Putra Malaysia, 43400 UPM Serdang, Selangor, Malaysia*
[b]*Advanced Materials and Nanotechnology Laboratory, Institute of Advanced Technology (ITMA), Universiti Putra Malaysia, 43400 UPM Serdang, Selangor, Malaysia*
[c]*Department of Chemistry, Faculty of Science, Universiti Putra Malaysia, 43400 UPM Serdang, Selangor, Malaysia*
[d]*Faculty of Applied Science, Universiti Teknologi MARA, 40450 Shah Alam, Selangor, Malaysia.*

TiO_2 nanotubes (TNT) have attracted considerable attention due to large specific surface area in a small geoetrical area and fewer interfacial grain boundaries. However, thermal stability and crystalline phase of TNT greatly affects their potential applications in the areas of photocatalysis, optoelectronics and gas sensing. Thus, thermal stability and phase transition of highly ordered TNT via calcination from 200-800 °C were studied in open air atmosphere. The results indicated that the as-anodized TNT is amorphous and transformed to anatase phase at 300 °C. Crystallization of anatase phase increases on elevating calcination temperature and rutile phase co-existed at 500 °C. No discernable changes in the nanotubes dimensions were found and TNT is thermally stable up to temperature lower than 600 °C, above which significant sintering of TNT occurred. At 800 °C, grain growth and oxidation of Ti resulted in completely collapsed of TNT to dense rutile crystallites. Photoelectrochemical response of calcined TNT enhanced substantially with respect to that of as-anodized samples and gradually increased with elevating temperature up to 500 °C after which they decreased, which was probably ascribed to changes in phase structural and morphological properties of TNT.

(Received June 14, 2012; Accepted December 20, 2012)

Keywords: Nanostructures, oxides, crystallisation, heat treatment

1. Introduction

Titanium dioxide (TiO_2) is a semiconductor material that has attracted tremendous attention in the last few decades owing to its remarkable properties including chemical stability, corrosion resistance, biocompatibility and specific ion intercalation properties. Apart from this, achieving high surface area without employing large geometrical area of TiO_2 is of interest of scientific community due to its technologically related application such as in water splitting, gas sensing, optoelectronics, photoelectrocatalysis, photovoltaic cell, electrochemical biosensing and other fields [1-5]. Among the one dimensional (1D) TiO_2 nanostructures (e.g. nanowires, nanorods and nanotubes), nanotubes have been studied extensively as they possess high surface area than other 1D nanostructures resulting from the hollow channel structures. Furthermore, vertically

---

[*] Corresponding author: Email address: zulkar@science.upm.edu.my

oriented and highly ordered TiO_2 nanotubes (TNT) of crystalline nature make them attractive to electron percolation pathways for charge transfer between interfaces [6].

The amorphous and crystalline nature of TNT varies with anodization parameters. For instance, crystalline TNT could be obtained by using comparable high applied voltage or employing higher bath temperature during electrochemical anodization [7,8] or by calcination the as-anodized amorphous TNT between 300-500 ^oC. Even though crystalline TiO_2 is essential to be utilized in certain applications, its structural stability can be greatly affected especially when crystallization and/or phase transformation occurs at elevated temperature. Structure and morphology instability is more pronounced when involving nanostructured materials with high surface area, as they are prone to solid state sintering and subsequently collapse of the structure. Therefore, crystalline nature, stability of crystalline phase and thermal stability of TNT structure need to be examined before TNT can be utilized for different application such as in catalysis [9], high temperature gas sensor [10] and dye-sensitized solar cells [4]. Even though several studies have been conducted to investigate the thermal effect on the structural and phase transition of TiO_2, similar studies on the influence of thermal treatment on resulting photoresponse of highly ordered TNT are still limited. Thus, in this paper, we have subjected TNT of 400 nm in tube length synthesized via electrochemical anodization to high temperature calcination, up to 800 ^oC in open air atmosphere to elucidate its thermal stability, structural transformation and photoelectrochemical response.

2. Experimental

2.1 Preparation of TiO_2 nanotubes

Ti foil (99.7 % purity, Sigma Aldrich) with a thickness of 0.127 mm was first cut into small rectangular size of 10 mm × 25 mm. The pure Ti foil was degreased by sonicating in acetone, isopropanol and deionized (DI) water, for 15 minutes each followed by chemically etched in 6 M HNO_3 for 10 minutes to form a fresh smooth surface. Then, the Ti foil was rinsed with excess DI water followed by drying in air. Electrochemical anodization of Ti was carried out in a dual-electrode chamber cell, in which the clean Ti foil with an area of 10×15 mm^2 immersed in the electrolyte was employed as the anode and a high density graphite electrode as the cathode. All anodization experiments were conducted at room temperature in 0.15 M NH_4F adjusted to pH 4 using H_2SO_4. Anodization was carried out at 20 V for 2 h using a DC power supply (Consort Mini, Cleaver Scientific Ltd). After anodization, the resulting films were immediately rinsed with deionized water and subsequently dried in air. In order to examine the crystallization and thermal stability of TNT, the samples were calcined at different temperatures, 200-800 ^oC in open air for 2 h with a heating rate of 2 ^oC/min. The same heat treatment was carried out on pure Ti plate as blank.

2.2 Characterization of as-anodized and calcined TiO_2 nanotubes

The phase composition and crystalline structure of TNT films were determined by X-ray diffraction (XRD, Shimadzu D6000) using a diffractometer with Cu K_α radiation ($\lambda = 1.5406$ Å) over the 2θ range of 20-60^o. The surface morphology of the as-anodized and calcined films was acquired by a field-emission scanning electron microscope, FESEM (Zeiss SUPRA 40 VP, Germany) operating at electron beam voltage of 5 kV and quantitative measurements were done using image analysis software (Image J). FESEM images were taken from at least three different locations on each sample to ensure that measurements of geometrical aspect (tube diameter and wall thickness) of TNT were representative. In order to obtain the thickness of the nanotube layer, direct cross-sectional images were taken from mechanically bent samples. At least five measurements of the cross section were taken from different location to ensure the measurements reflected the actual TNT layer thickness (tube length).

Photocurrent measurements were performed in 10 ppm methyl orange solution with 0.1 M KCl as supporting electrolyte in a conventional three-electrode cell. The synthesized TNT was employed as the working electrode, a platinum wire as the counter electrode, and Ag/AgCl as the reference electrode. The photocurrent was measured with a scanning potentiostat (μ-III AUTOLAB) under chopped irradiation from 120 V 300 W halogen lamp during a voltage sweep from +2.0 to –0.2 V with the sweep rate of 20 mV/s.

3. Results and discussion

XRD patterns of as-anodized and TNT calcined at 200-800 °C are shown in Fig. 1. It is evidently that the as-anodized sample (before calcination) and TNT calcined at 200 °C show only diffraction peaks of Ti substrate (JCPDS No. 44-1294) as shown in Fig. 1(a-b). This indicated the amorphous nature of both samples. However, crystallization in amorphous TNT to anatase occurs at 300 °C as a distinct peak was observed at 25.4^{o}, which was well indexed to anatase phase (JCPDS No. 21-1272) as shown in Fig. 1(c).

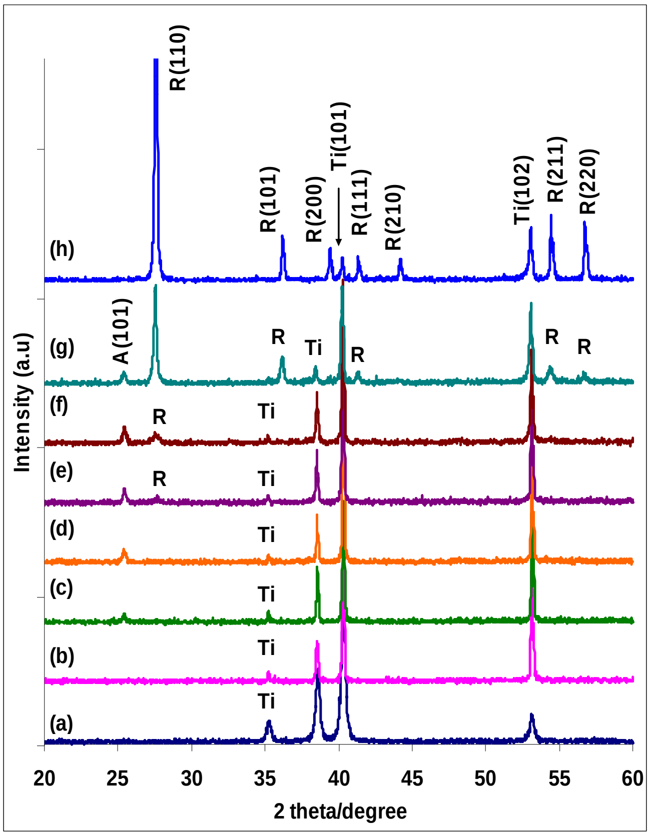

Fig. 1. XRD patterns of (a) as anodized TNT and calcined TNT at (b) 200 °C (c) 300 °C (d) 400 °C (e) 500 °C (f) 600 °C (g) 700 °C (h) 800 °C for 2h in open air atmosphere. A, R and Ti represent anatase, rutile and titanium, respectively.

This observation is in accord with the work reported by Varghese et al. that the crystallization of as-anodized amorphous TNT to anatase phase start approximately at 280 °C under dry oxygen atmosphere [11]. For TNT calcined at 400 °C, only anatase TiO_2 can be observed as shown in Fig. 1(d). Moreover, the relative intensity of anatase peak increases with elevating the calcination temperature from 300 to 600 °C, suggesting that the crystallinity of TNT was enhanced at higher calcination temperature. However, at 500 °C, a minor peak at 27.4^{o} is observed which was assigned to rutile (110) phase (JCPDS No. 21-1276); indicating anatase and rutile phase co-existed at temperature as low as 500 °C (Fig. 1(e)). This observation, however, is somewhat different from the previous findings of other researchers. Tian et al. [12] and Li et al. [13] observed the existence of rutile phase at much higher calcination temperature of 600 °C. Even though the reported TNT length in their works is 300 and 530 nm, respectively which is similar to our work (400 nm), however, electrochemical condition (electrolyte composition and anodization duration) used in synthesizing TNT and thus the resulting geometrical aspect of TNT are different, suggesting that TNT length is not solely the critical factor in phase transformation process.

As shown in Fig. 1(g), rutile (110) peak became predominant when TNT was calcined at 700 °C. In addition, the relative intensity of this peak increases with respect to anatase (101) peak. At 800 °C, the relative intensity of anatase peak greatly diminished and complete phase transformation from anatase to rutile phase occurred (Fig. 1(h)). This temperature, however, is much higher than previously reported results thus far for short nanotubes, where complete transformation to rutile occurs at 680 °C [11]. It can also be observed from Fig. 1 (h) that the diffraction peak from the Ti support decreases, being accompanied by a rapid increase in rutile intensity, indicating that probably there is a direct phase transformation from Ti to rutile. Also, work reported by Cai et al. [13] revealed that the constraint imposed by the nanotube walls prevent nucleation of larger rutile crystals until is reached a temperature where there is enough energy to cause the rupture of nanotube walls and thus collapse of nanotube structure and formation of larger rutile crystallites. This phenomenon is confirmed by XRD study of sample calcined at 800 °C, which shows the existence of only rutile phase.

From the XRD data, the weight fraction of rutile phase, W_R could be calculated according to a method reported by Zhang and Banfield [15], using the relation $W_R = I_R/(0.884I_A+I_R)$ where I_R represents the relative intensity of the rutile phase (110) peak and, I_A the relative intensity of anatase (101) peak. The rutile phase content in the sample calcined at 500, 600 and 700 °C were 17.7%, 49.9% and 95.8%, respectively. In order to confirm that the changes in phase crystallization are originated from TNT and not from the Ti substrate, the same heat treatment was performed to bare Ti substrate without TNT. Fig. 2 shows the XRD patterns of pure Ti without TNT with no heat treatment and samples that calcined at 500 and 600 °C. It is obvious that same diffraction pattern (only reflection of Ti peaks) is being observed for bare Ti and sample calcined at 500 °C (Fig. 2(a) and 2(b)). Rutile phase emerges when calcination temperature is further increased to 600 °C (Fig. 2(c)), which was not the case for TNT film calcined at 500 °C where both anatase and rutile (110) phase could be observed (Fig.1 (f)). The absence of the anatase phase in the oxidized Ti substrate is consistent with an accelerated phase transformation to rutile in the presence of a large number of oxygen vacancies [16, 17]. From a chemical thermodynamic point of view, the formation of rutile TiO_2 is favorable, as the Gibbs energy of formation for rutile ($\Delta_f G^o_{m,298K} = -888.67$ kJ/mol) is lower than that of anatase ($\Delta_f G^o_{m,298K} = -883.65$ kJ/mol). Hence, it is apparent that part of the rutile phase revealed in XRD patterns of calcined TNT is originated from the Ti substrate. The result also indicates that phase transformation of TNT (from amorphous to anatase then to rutile) occurred at elevated temperature.

As specific calcination temperatures and calcination rates can have an effect on the crystallite size, the variation of anatase and rutile crystallite size with temperature was calculated using the Scherrer equation, $D = 0.9\lambda/\beta \cos \theta$, where λ is the wavelength of Cu K_α radiation (1.5418 Å), 0.9 is the Scherrer constant, θ is the Bragg reflection angle, and β is the full width at half-maximum intensity of the anatase (101) peak or rutile (110) peak. Fig. 3 shows the variation of anatase (101) and rutile (110) crystallite sizes of calcined TNT as a function of calcination temperature. It can be seen that the average size of anatase grains decrease with an increase in calcination temperature, while the rutile grains size progressively increase after its nucleation from 500 to 800 °C. This indicates that at temperature above 500 °C, large anatase grains (in the tube-support interface region) transformed into rutile with smaller grains (in the nanotube walls) remained anatase.

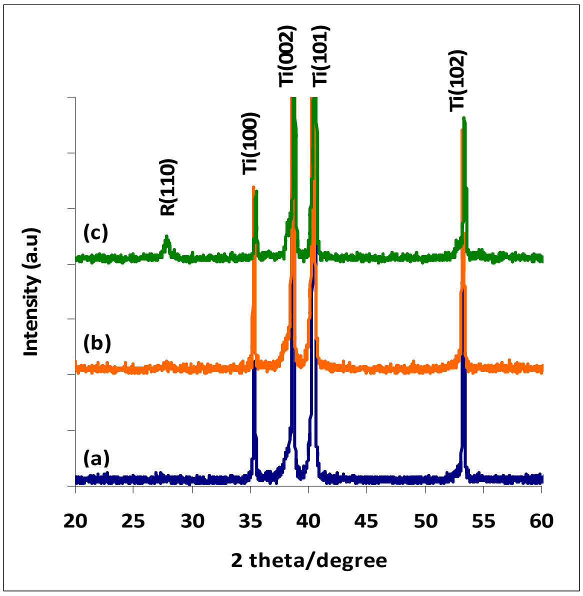

Fig. 2 XRD patterns of pure titanium without TNT (a) no heat treatment (b) calcined at 500 °C and (c) calcined at 600 °C in open air atmosphere. R and Ti represent rutile and titanium, respectively.

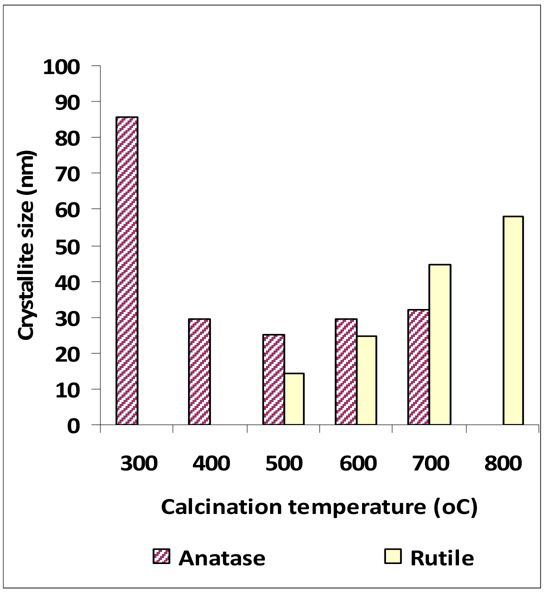

Fig. 3 Variation of anatase and rutile crystallite size of calcined TNT as a function of calcination temperature

It is believed that when TNT is subjected to heat treatment, crystallization of structure to anatase phase takes place both in the nanotube walls and the interface region between nanotube and the underlying Ti support [11]. As temperature rises, larger anatase crystallites were converted into rutile, as sufficient volume is available in the tube-support interface region during the growth and nucleation process [18]. However, this transformation is inhibited due to the constraints imposed by the walls leaving smaller anatase crystallites in the nanotube walls unaffected. Nevertheless, as reported by Varghese et al. [11], transformation of anatase to rutile eventually occurs in the walls when anatase crystallites in the wall meet rutile crystallites in the interface region forming larger rutile crystallites.

Fig. 4 depicts the FESEM images of as-anodized and calcined TNT at temperature ranging from 500 to 800 °C. It is apparent that the as-anodized TNT is uniform over the entire Ti substrate (inset in Fig. 4 (a) shows the high magnification image of this sample). As shown in Fig. 4(b), the sample exhibits tubular characteristic in vertical direction to Ti surface. This indicates the formation of well-ordered nanotube arrays with opened mouth and closed bottom (inset in Fig. 4(b)). The TNT is found to have average outer diameter of 75±8 nm with average wall thickness of 16±4 nm and tube length of 400±17 nm. For TNT calcined at 300, 400 and 500 °C, no discernible changes of pore diameter and wall thickness were observed and ordered nanotubular microstructures were well maintained. This result indicates that the fabricated TNT has excellent thermal stability as depicted in Fig. 4(c). Apart from calcination temperature, it is believed that calcination time might also affect the thermal stability of TNT. As calcination process involves mass transfer, a prolonged calcination time might favor more sintering and eventually leads to structural changes of TNT. As shown in Fig. 4(d), nanotubular structure is retained even after calcination for 6 h at 500 °C.

However, upon calcination at 600 °C, the inner diameter decreased to 59±7 nm, which is ascribed to the shrinkage of pores (Fig. 4(e)). At the same time, nanotube wall thickness increased from 16 to 20 nm. As shown in Fig. 4 (f), a thick oxide layer also gradually grows between the TNT and underlying Ti substrate resulting in the shortening of the nanotube length to 315±8 nm. This finding is in good agreement with the data in literature [19, 20]. An increase in wall thickness accompanied with a decrease in tube length is expected. This result also indicates that microstructure of TNT starts to deteriorate upon calcination at 600 °C. Such morphology change is favorable as nanostructured materials, which possess high surface area, is generally thermodynamically metastable. Therefore, TNT is prone to solid state sintering at high temperature calcination. This subsequently leads to grain growth, densification and increase in tube wall thickness. As a result, specific surface area and the total surface energy will be reduced.

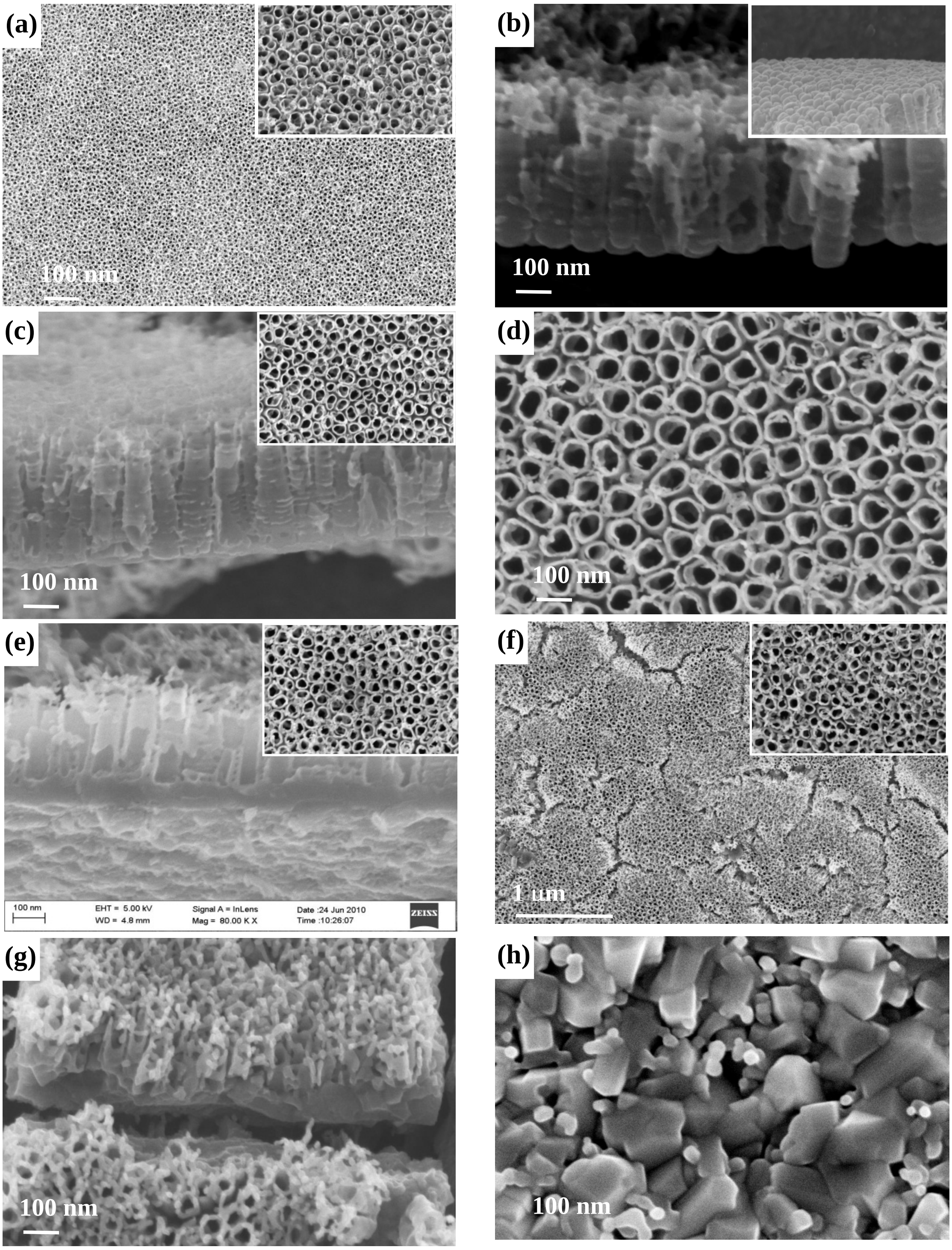

Fig. 4. FESEM images of TNT calcined at various temperatures: (a) top view, (b) cross sectional view of as-anodized TNT and (c) cross sectional view for TNT calcined at 500 °C for 2h (d) top view of TNT calcined at 500 °C for 6 h (e) cross sectional view of TNT calcined at 600 °C (f) top view, (g) cross sectional of TNT calcined at 700 °C (h) top view of TNT calcined at 800 °C. The inset in (a) and (f) show the high magnification view, inset in (c) and (e) show the top view of the corresponding samples. Inset in (b) shows the bottom view of as-anodized TNT.

It is worth mentioned that large parts of the nanotubular structure is retained even upon calcination at 700 °C. This observation can account the existence of anatase (101) peaks in the XRD patterns for samples calcined at 300-700 °C (Fig. 1) as it is believed that the anatase crystallites form within the tube walls [11, 16]. As shown in inset of Fig. 4(f), no significant coalition of nanotube wall is found which is not reported elsewhere previously. Nuepane et al. [21] observed coalition of tube wall forming wormlike pattern when TNT film is calcined at 500 °C. However, surface cracking with disordered nanotubes can be observed when calcination temperature is further increased to 700 °C (Fig 4(f)) whereas Tian et al. [13] observed similar phenomenon when TNT was calcined at as low as 600 °C.

In addition, it can be seen from the cross sectional view of sample calcined at 700 °C that the length of nanotubes decreases dramatically to about 200±10 nm and the oxide layer grows thicker between the nanotube arrays and the Ti substrate as shown in Fig. 4 (g). Yang et al. [22] also reported similar findings in their work on TNT with tube length of 4 µm. Apart from surface cracking, careful inspection of the FESEM image of sample calcined at 700 °C reveals small protrusions started to emerge from the underlying titanium substrate. This protrusions are believed to be the major cause of film degradation above this temperature (Fig. 4(f)) [10]. Nanotubular structure was destroyed to a great extent and completely collapses, leaving dense rutile crystallites when calcination temperature was further increased to 800 °C (Fig. 4(h)). When the as-anodized TNT was subjected to calcination at different temperatures, the color of the samples gradually changed, from light gray green for the as-anodized TNT, to the light yellow for TNT calcined at 500 °C and to darker gray for TNT calcined at 700 °C.

3.1 Photoelectrochemical response of TiO_2 nanotube arrays

Crystalline nature and stability of crystalline phase present in TNT can greatly influence their photoelectrochemical response. Therefore, phototransients were measured at 1 V versus Ag/AgCl with a 10 seconds light pulse for the as-anodized and 500 °C calcined TNT from halogen lamp (120 V 300W) as shown in Fig. 5. Information about the electron transport in TNT could be revealed from this phototransients measurement.

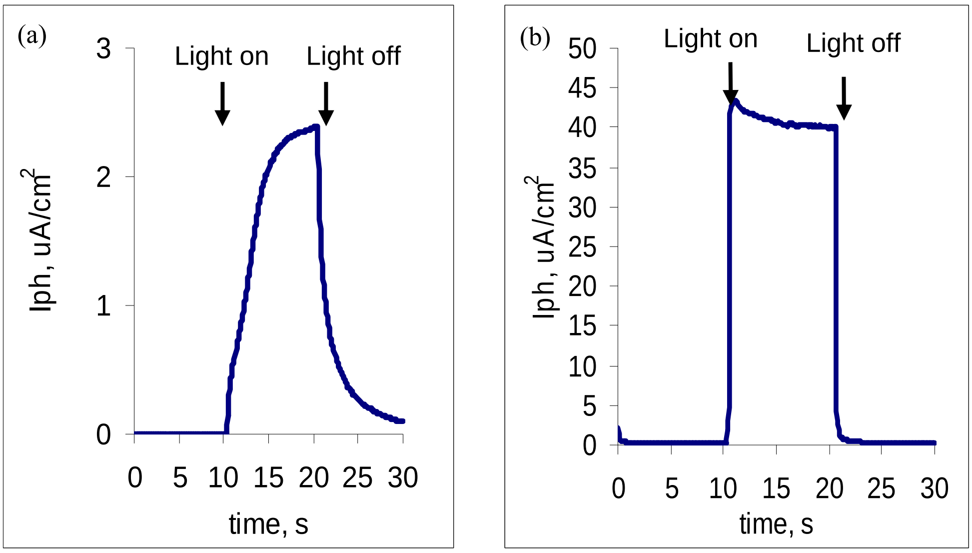

Fig. 5. Phototransients measurement from halogen lamp at 1 V versus Ag/AgCl with 10s light pulse for a) as-anodized TNT and (b) TNT calcined at 500 °C for 2h in open air atmosphere. Phototransients measurement was done using 10 ppm methyl orange solution with 0.1 M KCl as supporting electrolyte.

Slow increase in photoresponse to a very low photocurrent magnitude about 2 uA/cm^2 for as-anodized TNT (Fig. 5(a)) indicates the presence of a high number of defects which can act as traps and recombination centers for the photogenerated charge carriers. Low photoresponse in as-anodized TNT is originated from the tube bottom as photogenerated charge carriers in the tube walls recombine at defects before they reach the tube bottom [6]. Substantial enhancement in photoresponse is observed when TNT is subjected to calcination at 500 ^{o}C (Fig. 5(b)) ascribed to lose of trap filling phenomenon and transformation of amorphous TNT to crystalline anatase and rutile phase. Apart from the enhancement of photoresponse for calcined TNT, different phototransient shapes observed also suggests that a different electron driving mechanism is involved in which diffusion process rather than drift is dominant in as-anodized TNT [23].

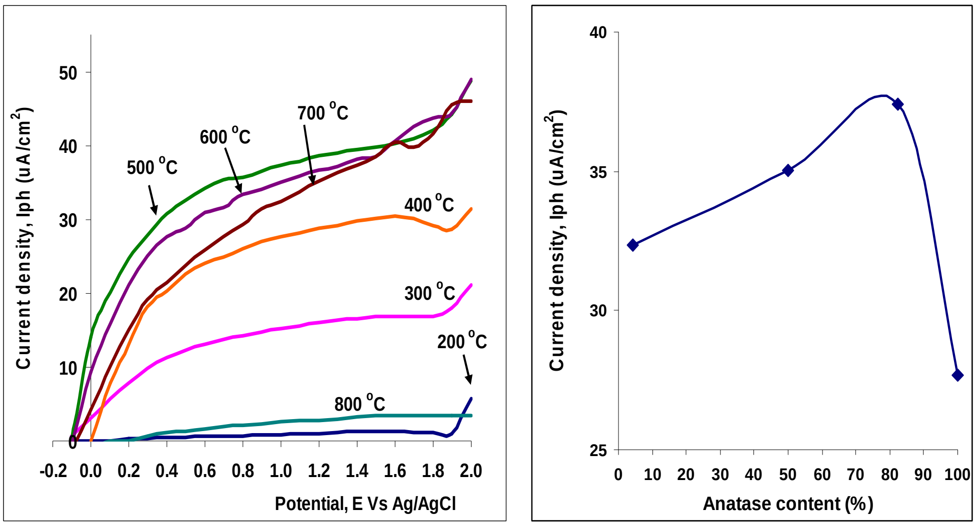

Fig. 6 (a) Photoresponse of TNT calcined at various temperatures in open air atmosphere (b) Photoresponse of TNT at 1.0 V vs. Ag/AgCl versus anatase content in TNT. Photoresponse measurement was done in 10 ppm methyl orange solution with 0.1 M KCl as supporting electrolyte from 300 W halogen lamp at scan rate of 20 mV/s.

Fig. 6 (a) shows the photocurrent response of calcined TNT at various temperatures ranging from 200-800 ^{o}C. TNT calcined at 200 ^{o}C demonstrated almost negligible photoresponse and this is expected as it exhibits amorphous structure from the XRD study. However, photocurrent responses of calcined TNT increase with elevating calcination temperature from 300 to 500 ^{o}C. Considering the fact that both TNT samples calcined at 300 and 400 ^{o}C exhibit pure anatase phase as revealed by XRD study (Fig. 1(c) and (d)), the photocurrent response of the latter sample is higher than that of the former. This probably ascribed to better crystallization of TNT at higher heat treatment temperature.

It is noteworthy that TNT calcined at 500^{o}C demonstrated highest photocurrent response, which is probably due to co-existence of mix anatase and rutile phase. Moreover, it is observed that TNT with a mixture of anatase and rutile phase (TNT calcined at 500, 600 and 700 ^{o}C) demonstrated relatively higher photocurrent response with respect to that of pure anatase (TNT calcined at 300 and 400 ^{o}C) or rutile phase (TNT calcined at 800 ^{o}C). This result indicates that TNT with mix anatase and rutile phase shows a lower electron-hole recombination and higher photoelectron transfer efficiency, which could eventually benefit photocatalytic reaction [24]. Even though the mix phase TNT demonstrated higher photocurrent response than that of pure phase, the photocurrent increases with increasing anatase content up to 82% in mix phase TNT as shown in Fig. 6 (b). This is due to anatase owns a higher charge carrier mobility of 80 cm^{2}v^{-1}s^{-1} which is 89 times faster than that of rutile phase [25]. Thus, mix phase TNT with major anatase content is expected to demonstrate higher photoresponse.

However, when comparing the photocurrent response of TNT calcined at 500, 600 and 700 ^{o}C, photocurrent decreases with elevating temperature. This could be attributed to the presence of substantial rutile weight fraction from 18% for TNT calcined at 500 ^{o}C to about 96% for TNT calcined at 700 ^{o}C. As rutile phase is generally associated with fast charge carriers recombination rate, low photocurrent is observed for sample with high rutile weight fraction. In addition, increasing temperature from 600 to 700 ^{o}C initiates the deteriorating of nanotubular structure owing to the formation of rutile crystallites in the nanotube wall. Therefore, morphological disorder will create more defects, which is expected to lead to slower electron transport and higher recombination rates. This result also implies that there should be a balance between crystal phase and nanotubular microstructure for achieving high photoelectrochemical performance of TNT. Photocurrent decreases dramatically when TNT is subjected to high calcination temperature (above 800 ^{o}C) as nanotubular configuration completely collapsed leaving dense rutile crystallite and this result in great reduction of surface area causing lower overall incident photon absorption. Therefore, factors such as crystalline phase, morphological properties and surface area can greatly influence the photoelectrochemical response of TNT.

4. Conclusions

In summary, vertically oriented and highly ordered TNT films were fabricated by simple anodization of Ti foil in aqueous electrolyte containing NH_4F and the effect of post thermal treatment on TNT was investigated. Results show that there is only anatase phase below the calcination temperature of 400 ^{o}C and rutile phase starts to emerge at 500 ^{o}C. The TNT is stable up to temperature lower than 700 ^{o}C and high temperature calcination (above 600 ^{o}C) resulted in a change of morphology and geometrical aspects of TNT (diameter, wall thickness and tube length). Higher calcination temperatures increase the rutile content and thickness of the barrier layer that could interfere with charge transfer to the back contact, but also improve the crystallinity of the nanotubes. As photocurrent response is strongly influenced by crystal phase present and nanotubular microstructures, calcination of TNT at 500 ^{o}C appeared to be the most favorable condition to retain the nanotubular structure with desired crystal phase and photoelectrochemical properties. Thus, controlling the phase composition through calcination is a simple and attractive way to tune the overall photoelectrochemical performance of TNT.

Acknowledgements

The authors are thankful to the Faculty of Applied Science, Universiti Teknologi MARA for helping in FESEM. The Fundamental Research Grant Scheme (FRGS) grant received (Grant no: 01-04-10-859FR) from the Ministry of Higher Education is also gratefully acknowledged.

References

[1] J. M. Macak, H. Tsuchiya, A. Ghicov, K. Yasuda, R. Hahn, S. Bauer, P. Schmuki, Curr. Opin. Solid State Mater. Sci. **11**(1-2), 3 (2007).
[2] Y. Zhang, W. Fu, H. Yang, Q. Qi, Y. Zeng, T. Zhang, R. Ge, G. Zou, Appl. Surf. Sci. **254**, 5545 (2008).
[3] Y. Liu, B. Zhou, J. Bai, J. Li, J. Zhang, Q. Zheng, X. Zhu, W. Cai, Appl. Catal., B-Environ. **89**, 142 (2009).
[4] P. Charoensirithavorn, Y. Ogomi, T. Sagawa, S. Hayase, S. Yoshikawa, J. Cryst. Growth. **311**, 757 (2009).
[5] S. Liu and A. Chen, Langmuir **21** (18), 8409-8413 (2005).
[6] A. Ghicov, P. Schmuki, Chem. Commun. **2009** (20), 2791 (2009).
[7] Y. Xie, L. M. Zhou, H. Huang, Mater. Lett. **60**, 3558 (2006).
[8] X. Xiao, K. Ouyang, R. Liu, J. Liang, Appl. Surf. Sci. **255**, 3659 (2009).

[9] H. C. Liang, X. Z. Li, J. Hazard. Mater. **162**, 1415 (2009).

[10] G. K. Mor, O. K. Varghese, M. Paulose, K. G. Ong, C. A. Grimes, Thin Solid Films **496**, 42 (2006).

[11] O. K. Varghese, D. Gong, M. Paulose, C. A. Grimes, E. C. Dickey, J. Mater. Res. **18**, 156 (2003).

[12] G. Li, Z. Q. Liu, J. Lu, L. Wang, Z. Zhang, Appl. Surf. Sci. **255**, 7323 (2009).

[13] T. Tian, X. Xiao, R. Liu, H. She, X. Hu, J. Mater. Sci. **42**, 5539 (2007).

[14] Q. Cai, M. Paulose, O. K. Varghese, C. A. Grimes, J. Mater. Res. **20**, 230 (2005).

[15] H. Zhang, J. Banfield, J. Phys. Chem. B **104**, 3481 (2000).

[16] K. Zhu, N. Neale, A. Halverson, J. Kim, A. Frank, J. Phys. Chem. C **114**, 13433 (2010).

[17] C. C. Ting, S. Y. Chen and D. M. Liu, J. Appl. Phys. **88**, 4628 (2000).

[18] P. Gouma, M. Mills, J. Am. Ceram. Soc. **84**, 619 (2001).

[19] P. Xiao, D. Liu, B. B. Garcia, S. Sepehri, Y. Zhang, G. Cao, Sens. Actuators, B: Chemical **134**, 367 (2008).

[20] J. Zhao, X. Wang, T. Sun, L. Li, J. Alloys Compd. **434-435**, 792 (2007).

[21] M. P. Neupane, I. S. Park, M. H. Lee, T. S. Bae, F. Watari, Biomed. Mater. Eng. **19**, 77 (2009).

[22] Y. Yang, X. Wang, L. Li, J. Am. Ceram. Soc. **91**, 632 (2008).

[23] A. Ghicov, H. Tsuchiya, J. Macak, P. Schmuki, Phys. Status Solidi (A) **203**, R28 (2006).

[24] H. Zhuang, C. Lin, Y. Lai, L. Sun, J. Li, Environ. Sci. Technol. **41**, 4735 (2007).

[25] S. Bakardjieva, J. Šubrt, V. Šengl, M. J. Dianez and M. J. Sayagues, Appl. Catalysis, B: Environ. **58**, 193 (2005).